TRENDS IN SCIENCES 2026; 23(4): 11900
https://doi.org/10.48048/tis.2026.11900 RESEARCH ARTICLE

Co-Sputtering Ti-Ag-N Films: Structure, Wettability, and Antibacterial Properties

Ihwanul Aziz*, Azza Alifa Muhammad, Frida Iswinning Diah, Agus Dwiatmaja, Fajar Sidik Permana, Suharni Suharni, Kurnia Wibowo, Taufik Taufik and Emy Mulyani

Research Center for Accelerator Technology, Research Organization for Nuclear Energy, National Research and Innovation Agency, South Tangerang, Indonesia

(*Corresponding author's e-mail: ihwa002@brin.go.id)

Received: 15 September 2025, Revised: 4 November 2025, Accepted: 14 November 2025, Published: 1 January 2026

Abstract

Incorporating silver (Ag) into titanium nitride (TiN) coatings is an effective strategy to enhance their structural integrity, mechanical strength, surface characteristics, and antibacterial activity. In this study, Ti–Ag–N coatings were deposited via DC magnetron sputtering using Ag plates with diameters of 0, 4, 6, and 8 mm. The resulting films were analyzed using XRD, SEM/EDS, hardness tests, and water contact angle measurements, while their antibacterial performance was tested against Staphylococcus aureus. Moderate Ag incorporation (Ag-6) yielded the best overall properties, improving crystallinity, producing a uniform Ag distribution, and increasing surface energy. This composition also demonstrated the highest hardness (179.24 VHN) and excellent wettability. Antibacterial tests confirmed that Ag-containing coatings - particularly Ag-6 - suppressed bacterial growth by up to 99.99%, mainly due to controlled Ag ion release and enhanced surface energy. These results indicate that optimizing Ag content effectively balances durability, functionality, and antibacterial performance, making Ti–Ag–N coatings promising candidates for biomedical and advanced engineering applications.

Keywords: Antibacterial coatings, Biomedical applications, Contact angle, DC sputtering, Structural properties, Surface wettability, Ti–Ag–N thin films

Introduction

Bacterial adhesion and surface colonization remain major challenges across various industries, particularly in medical devices and food packaging, where microbial contamination can threaten health, reduce product quality, and cause economic losses [1,2]. Materials used in these sectors such as food packaging, medical tools, dental and orthopedic implants, and water purification systems are constantly exposed to bacterial contamination [3]. Among these, food packaging is especially critical. Insufficient antibacterial protection can accelerate the growth of harmful bacteria, compromising food safety and shortening shelf life [4]. This not only affects overall food quality but also poses broader public health concerns [5]. This situation underscores the urgent need for innovative surface technologies that can effectively suppress bacterial growth and enhance consumer safety.

For decades, antibiotics have been the primary means of controlling bacterial contamination and ensuring food safety. However, excessive and uncontrolled use has led to the rise of multidrug-resistant (MDR) bacteria, diminishing the effectiveness of traditional antimicrobial strategies. As a result, researchers have turned to alternative, sustainable solutions particularly metal-based nanoparticles (NPs), nanocomposite coatings, and multifunctional thin films [4]. These approaches provide new opportunities to extend product shelf life, maintain food quality, and reduce microbial risks without depending solely on antibiotics.

Biofilm formation further complicates bacterial control. When bacteria adhere to a surface and secrete a protective extracellular matrix of polysaccharides, proteins, and DNA, they form biofilms that are far more resistant to antimicrobials and environmental stress than free-floating cells [5]. In food packaging, biofilms enable persistent contamination that is difficult to remove [6]. Preventing bacterial attachment and early biofilm formation is generally more effective than attempting to eliminate mature biofilms [7]. Surface morphology, physicochemical properties, and environmental conditions strongly influence these processes [7,8]. Therefore, modifying surface features through advanced coatings and nanocomposites offers a promising route to suppress biofilm development and improve food safety.

Key surface properties such as roughness, wettability, and nanoscale texture play central roles in bacterial adhesion. Wettability, often represented by contact angle, is particularly influential [9]. Generally, hydrophilic surfaces with low contact angles discourage bacterial attachment and enhance surface cleanliness. However, the relationship between wettability and adhesion is complex: Some studies report reduced adhesion on hydrophilic surfaces, while others observe the opposite [8]. This suggests that wettability should be assessed alongside other surface and environmental factors when designing antimicrobial materials.

Effective antibacterial coatings for food packaging must meet several criteria. They should inhibit bacterial adhesion and biofilm formation while maintaining safety, non-toxicity, and compliance with food safety standards [10]. In addition, they must exhibit broad-spectrum antibacterial activity, strong mechanical durability, and cost-efficiency to withstand the demands of packaging, storage, and distribution [11]. Achieving these characteristics requires multifunctional materials that balance performance, safety, and scalability.

Titanium (Ti) and its alloys are promising candidates due to their high strength, corrosion resistance, and excellent biocompatibility [12]. Incorporating silver (Ag) into Ti-based coatings further enhances antibacterial performance and surface functionality [8,13-16]. Silver is widely recognized for its strong, broad-spectrum antibacterial properties against both Gram-positive and Gram-negative bacteria, making it highly suitable for advanced food packaging applications [17]. Despite these advantages, the effects of Ag incorporation on nanoscale surface features such as roughness, wettability, and contact angle behavior are still not fully understood, especially in Ti–Ag–N thin films designed for multifunctional antibacterial coatings.

Several deposition methods have been developed to create thin films with tailored properties, including sol-gel, spin coating, anodic oxidation, physical vapor deposition (PVD), and electrodeposition [18,19]. Among these, magnetron sputtering stands out for its ability to produce smooth, dense, and uniform coatings with precise compositional control [12,20]. In this study, Ti–Ag–N thin films were fabricated via DC magnetron sputtering on SS316L substrates, using varying Ag plate diameters to adjust coating composition and properties. The films were systematically characterized in terms of structure, surface morphology, wettability, elemental composition, and antibacterial performance. This work aims to clarify the relationship between Ag incorporation, surface characteristics, and antibacterial activity, offering insights for the design of durable and efficient Ti–Ag–N coatings. Ultimately, the study proposes a practical route to develop high-performance antimicrobial surfaces that enhance food safety and prolong product shelf life.

Methodology

Materials and methods

TiN thin films with varying silver (Ag) atomic contents were synthesized using a reactive DC magnetron sputtering technique. The substrates consisted of single-side polished SS316L foils with dimensions of 10×10 mm^2 and a thickness of 0.9 mm. The chemical composition of the SS316L substrate, obtained from energy-dispersive X-ray spectroscopy (EDS) analysis, is presented in **Table 1**. High-purity titanium (Ti) disks (99.99%, Goodfellow) with a diameter of 50 mm and a thickness of 3 mm were used as sputtering targets. For silver doping, high-purity Ag foils (99.99%, Goodfellow) were prepared in 5 different diameters 5, 7.5, 10, 12.5 and 15 mm - with a constant thickness of 0.1 mm. Details of the sample codes and deposition parameters for the Ti-Ag-N films are summarized in **Table 2**.

The deposition process was conducted under an initial base pressure of 2.5×10^{-4} mbar and a constant

working pressure of 2×10^{-2} mbar. Prior to deposition, all substrates were sequentially cleaned in an ultrasonic bath using a mild detergent solution followed by ethanol for 10 minutes each to ensure complete surface decontamination. The Ti–Ag–N films were deposited using a reactive DC sputtering process with an optimized gas flow ratio of argon to nitrogen (Ar:N_2) at 80:20. During deposition, the discharge voltage and current were maintained at 5 kV and 10 mA, respectively. Optimization of the deposition parameters was performed based on the measured Vickers hardness values of the films, as illustrated in **Figure 1**. The Ag content within the coatings was precisely controlled by systematically varying the diameters of the Ag foils placed directly on the Ti target surface, enabling controlled doping without altering other sputtering conditions.

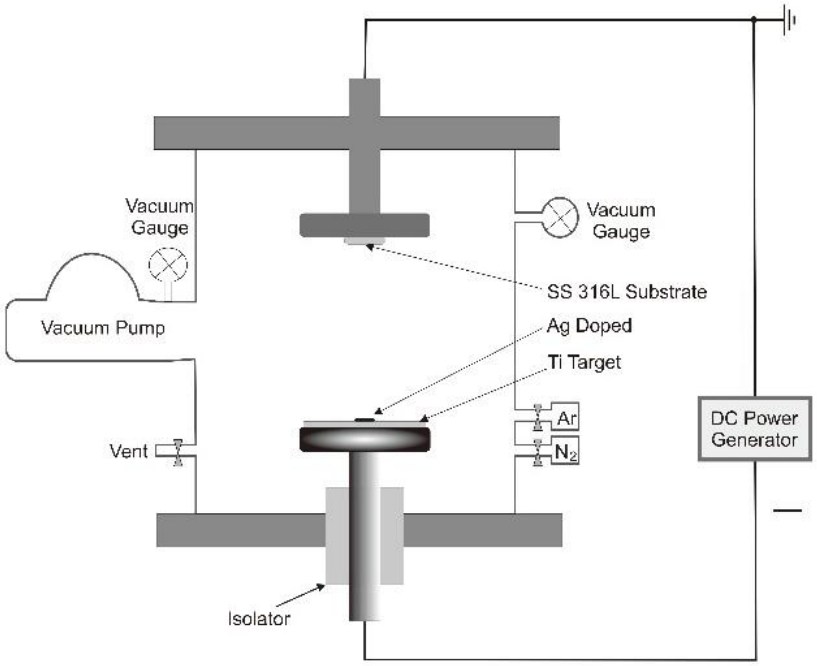

Figure 1 Schematic deposition Ti–Ag–N on SS 316L with co-sputtering method.

Structural and surface characterization of Ti–Ag–N Films

The surface morphology of the Ti–Ag–N coatings deposited on SS316L substrates was examined using a scanning electron microscope Hitachi. The elemental composition and variations in Ag content were analyzed using energy-dispersive X-ray spectroscopy (EDS). The crystalline structure of the films was characterized by X-ray diffraction (PANalytical), enabling phase identification and analysis of preferential growth orientations.

Mechanical characterization

The hardness of the Ti–Ag–N coatings was measured using a Vickers digital microhardness tester (Matsuzawa) under a constant load of 10 g with a dwell time of 10 s. Measurements were performed at ten randomly selected points on each sample, and the average Vickers hardness value (HV) was calculated to ensure statistical reliability.

Wettability (contact angle) measurements

The wettability of the Ti–Ag–N coatings was evaluated by measuring the static water contact angle on the sample surfaces. Contact angle measurements were performed using a VHX-5000 digital microscope equipped with an advanced CMOS sensor, capable of capturing high-resolution images at 50 frames per second. The VHX-5000 also integrates a high dynamic range (HDR) imaging algorithm, which enhances image contrast and minimizes overexposure or underexposure on unevenly illuminated surfaces. Furthermore, the device utilizes a super-resolution imaging mode combined with short-wavelength light and pixel-shift

technology, enabling a 25% improvement in spatial resolution with a magnification range from 0.1× to 5,000×.

Antibacterial activity assay

The antibacterial performance of the Ti–Ag–N films was evaluated against Staphylococcus aureus using a modified colony-forming unit (CFU) counting method. A bacterial suspension was prepared by inoculating a single colony into nutrient broth, followed by incubation under continuous shaking at room temperature until the bacterial concentration reached approximately 5×10^8 CFU/mL. Sterile SS316L plates coated with Ti–Ag–N films were placed in UV-sterilized Petri dishes and exposed to UV light for 15 min prior to testing. Subsequently, 50 μL of the bacterial suspension was carefully dropped onto the coated films and uncoated control samples. The Petri dishes were then incubated at 37 °C under ~90% relative humidity for 24 h.

After incubation, the samples were gently rinsed with 10 mL of phosphate-buffered saline (PBS) to remove non-adherent bacteria. Serial dilutions of the bacterial suspensions were prepared up to 10^5-fold using PBS. From each dilution, 0.1 mL of solution was spread onto nutrient agar plates using a Drigalski spreader under aseptic conditions. The plates were incubated at 37 °C for 24 h, after which the number of bacterial colonies was quantified using a colony counter. The antibacterial effectiveness (R) of the coatings was calculated using Eq. (1):

$$\text{Antimicrobial effectiveness: } (N0 - N)/N0\times100\% \quad (1)$$

where N0 represents the number of colonies on the control sample, and N represents the number of colonies on the Ti–Ag–N-coated sample.

Table 1 Chemical composition stainless steel 316L from EDS data.

Raw material	Fe (wt.%)	Cr (wt.%)	Ni (wt.%)	Mo (wt.%)	Others (wt.%)
SS 316L	70.45	17.05	10.44	1.94	0.12

Table 2 Deposition parameter of Ti–Ag–N films.

Sample code	Ag plate diameter (mm)	Deposition Time (min)
TiN	0	120
Ag-4	4	120
Ag-6	6	120
Ag-8	8	120

Results and discussion

The XRD patterns (**Figure 2(a)**) show cubic TiN phases, metallic Ag, and minor γ-Fe from the stainless-steel substrate. For undoped TiN, diffraction peaks appear at $2\theta \approx 36.7°$, 42.6°, and 61.8°, corresponding to the (111), (200), and (220) planes of TiN (ICDD PDF No. 38-1420) [21]. With Ag incorporation, new peaks emerge at $2\theta \approx 38.1°$, 44.3°, and 64.4°, indexed to metallic Ag (ICDD PDF No. 04-0783) [22]. Their increasing intensity, especially in Ag-8, indicates Ag crystallite growth and surface enrichment. Small peaks near $2\theta \approx 43.5°$ and 77.5° match γ-Fe planes (ICDD PDF No. 31-0619) [23], confirming substrate contributions. The narrower FWHM of Ag peaks compared to TiN suggests larger Ag crystallite sizes, consistent with Scherrer analysis [24]. Overall, these findings demonstrate that Ag atoms tend to form well-defined crystalline inclusions without significantly disrupting the TiN lattice, leading to the formation of TiN/Ag hybrid composites with improved structural and functional properties [15]. Such microstructural evolution is in strong agreement with recent studies [25] reporting enhancements in hardness, wear resistance, and biofunctionality when noble-metal nanoparticles are integrated into TiN-based coatings. Crystallite size and microstrain (**Figure 2(b)**) depend strongly on Ag content. Undoped TiN shows ~22.5 nm grains with low microstrain ($\sim2.1\times10^{-3}$). Adding small Ag (Ag-4)

increases size to ~24.8 nm and slightly reduces microstrain (~2.05×10⁻³), suggesting Ag promotes grain coarsening and reduces lattice defects [26]. The presence of distinct Ag peaks without shifts in TiN reflections, together with constant nitrogen levels from EDS, confirms that Ag does not enter the TiN lattice but segregates at grain boundarie.

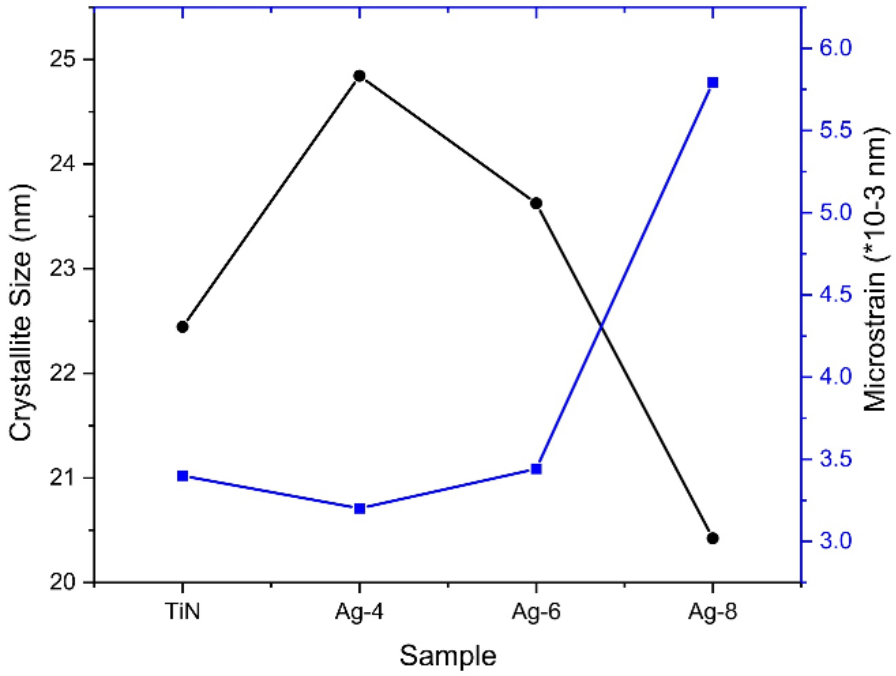

Figure 2 (a) XRD data fitted using Rietveld refinement; (b) Microstrain and crystallite size.

Table 3 Comparison of Experimental XRD Peaks with Reference Data

Phase	ICDD Card No.	hkl	2θ (Experimental)	2θ (Reference)
TiN	38-1420	(111)	36.7°	36.66°
TiN	38-1420	(200)	42.6°	42.62°
TiN	38-1420	(220)	61.8°	61.84°
Ag	04-0783	(111)	38.1°	38.12°
Ag	04-0783	(200)	44.3°	44.28°
Ag	04-0783	(220)	64.4°	64.43°
Austenite (γ-Fe)	31-0619	(111)	43.5°	43.52°
Austenite (γ-Fe)	31-0619	(220)	77.5°	77.49°

However, further increasing the Ag content (Ag-6) leads to a gradual reduction in crystallite size (~23.5 nm), accompanied by a noticeable rise in microstrain (~3.5×10⁻³ nm), implying the onset of Ag clustering and localized lattice mismatch between the TiN and Ag phases. At the highest Ag concentration (Ag-8), a pronounced decrease in crystallite size (~21 nm) is observed together with a sharp increase in microstrain (~5.9×10⁻³ nm), indicating phase segregation and significant lattice distortion induced by the accumulation of Ag-rich domains. The increase in microstrain at high Ag content (Ag-8) arises mainly

from lattice mismatch with Ag clusters, further aggravated by defects and residual stress. Similar trends have been reported in other Ag-doped nitride and chalcogenide systems, where low Ag content improves crystallinity and reduces residual stress, whereas excessive Ag promotes grain refinement and defect formation [27,28]. These findings confirm the existence of an optimal Ag content, where controlled Ag incorporation effectively enhances crystallite growth and minimizes lattice strain, while excessive Ag leads to microstructural disruption, which is consistent with previous studies on Ag-modified thin films [27].

Figure 3 shows that Ag content strongly influences the surface morphology of Ti–Ag–N films on SS316L. The undoped TiN coating displays a compact, fine-grained surface, consistent with XRD results indicating small crystallites and low microstrain (**Figure 2(b)**). With Ag-4, grains coarsen and the distribution broadens, while XRD confirms larger crystallites and slightly reduced microstrain. This suggests that Ag promotes heterogeneous nucleation, enhancing atomic mobility and reducing lattice defects. At Ag-6, the morphology becomes irregular with signs of agglomeration. The crystallite size decreases and microstrain rises, indicating strain accumulation from Ag clustering and lattice mismatch. For Ag-8, the surface shows large, irregular agglomerates and severe grain size variation. These features align with a sharp reduction in crystallite size and increased microstrain, pointing to phase segregation and structural distortion. Overall, low Ag levels enhance crystallinity and grain uniformity, whereas excessive doping destabilizes the microstructure - consistent with trends reported in other Ag-modified nitride and chalcogenide systems [29,30].

At higher Ag levels (Ag-6), microstructural instability becomes evident: XRD suggests strain buildup and decreased crystallite size, while SEM/EDS highlight Ag-rich agglomeration—behavior also reported in TiAlN films doped with Ag [31]. At the highest doping level (Ag-8), morphological degradation accelerates, with SEM showing roughened, inhomogeneous surfaces, while XRD indicates significant lattice distortion. This mirrors findings in decorative TiN-Ag coatings where surface roughness sharply increases beyond ~8 at% Ag [15]. Collectively, these real-world studies substantiate that low-to-moderate Ag doping can enhance crystallinity and grain structure, but excessive Ag induces phase segregation, elevated microstrain, and morphological instability underscoring the critical need to optimize Ag content for high-performance Ti–Ag–N coatings.

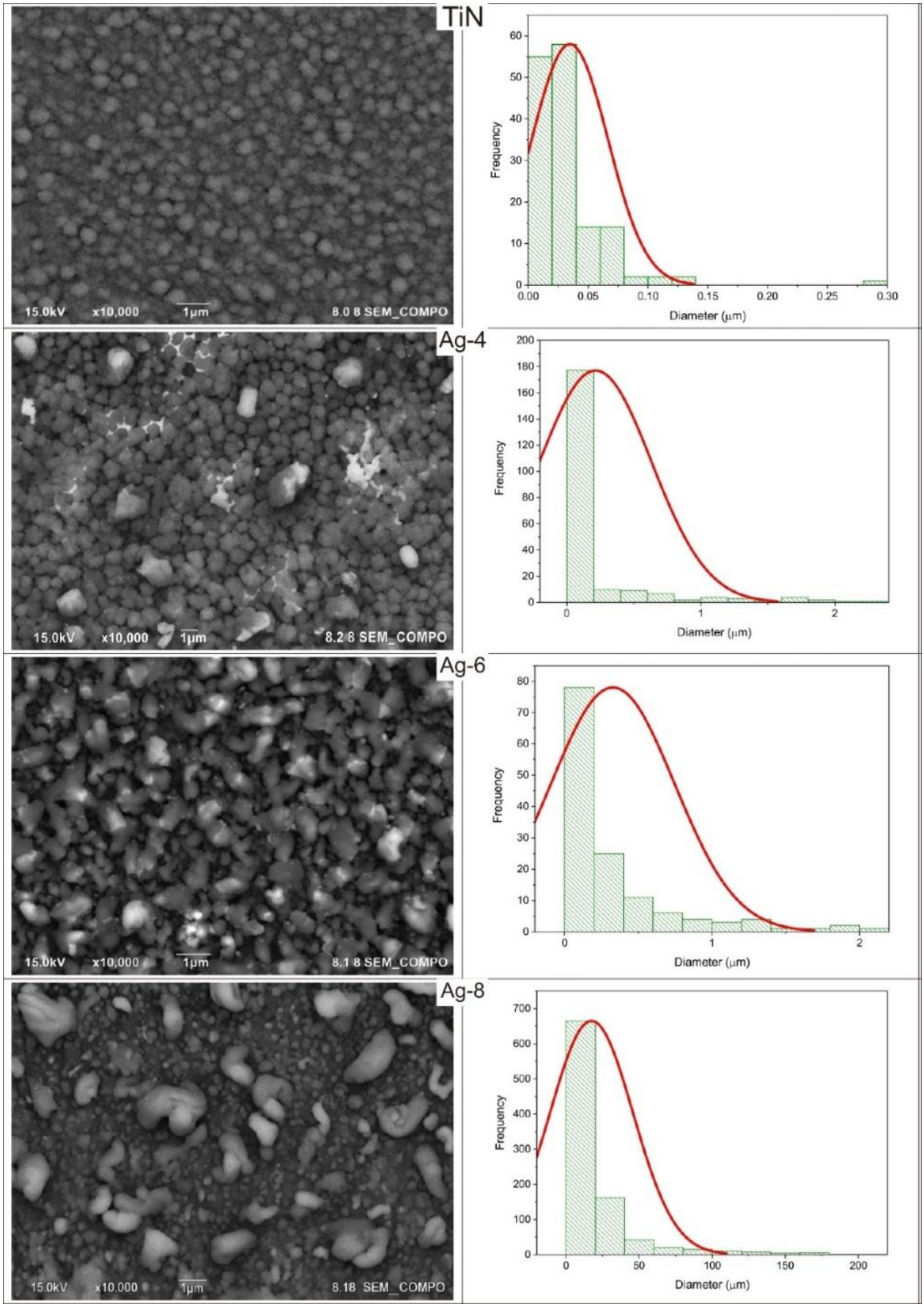

Figure 3 SEM Surface morphology and grain size distribution.

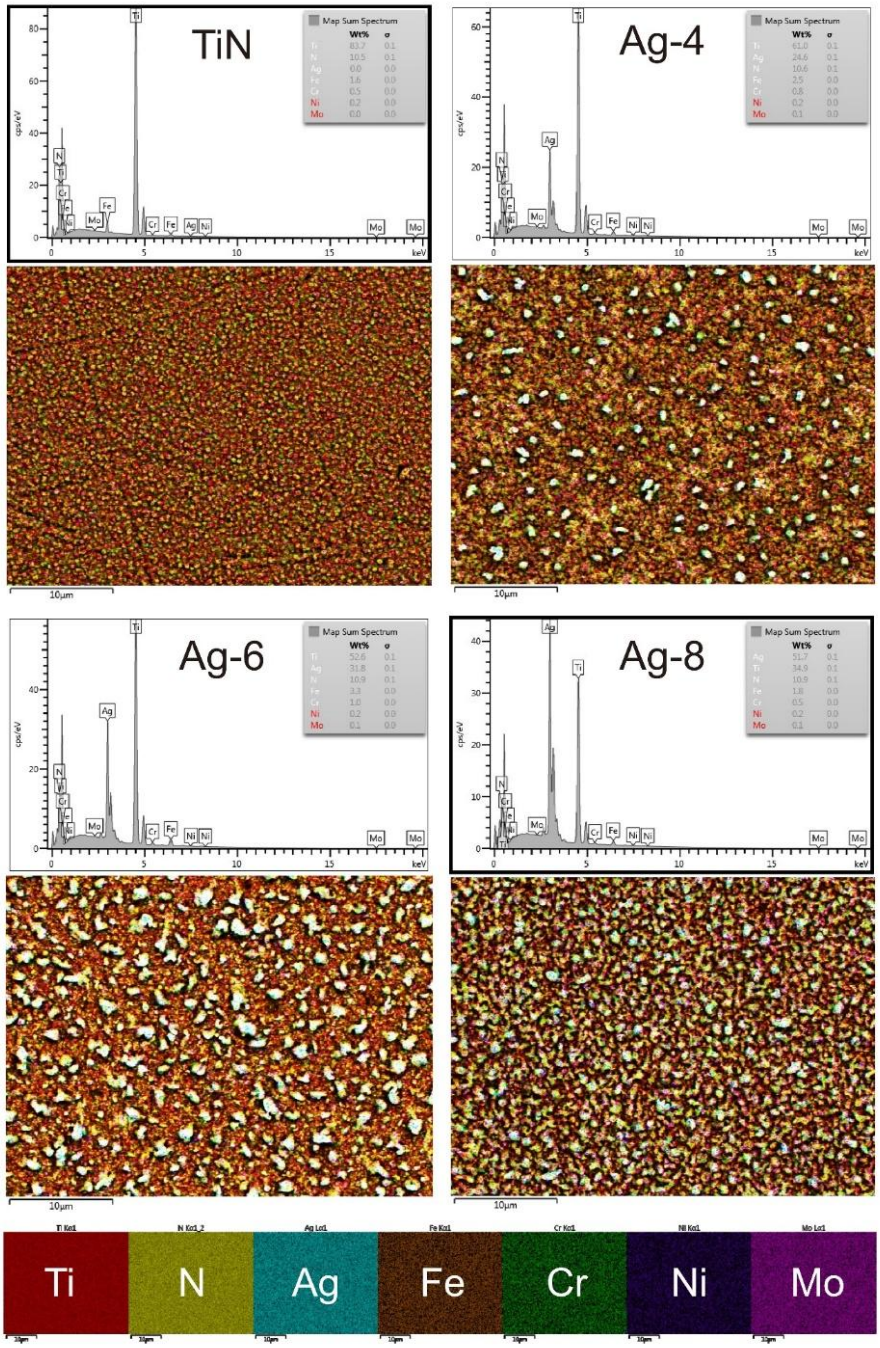

Figure 4 SEM-EDS elemental distribution mapping.

Figure 5 shows that silver content strongly alters the composition of Ti–Ag–N coatings. The undoped film consists mainly of Ti and N, confirming a near-stoichiometric TiN matrix. With Ag-4, silver appears in significant amounts while nitrogen remains stable, suggesting that Ag segregates at grain boundaries rather than integrating into the Ti–N lattice. At Ag-6 and Ag-8, silver fraction continues to rise as titanium decreases, while nitrogen stays nearly constant. This trend indicates progressive enrichment of Ag in metallic domains, consistent with previous reports of Ag-rich particles embedded within TiN matrices [15]. Overall, controlled Ag doping enables adjustment of the metal-to-nitride ratio, improving properties such as conductivity and antibacterial activity. However, excessive Ag promotes segregation that may compromise structural stability.

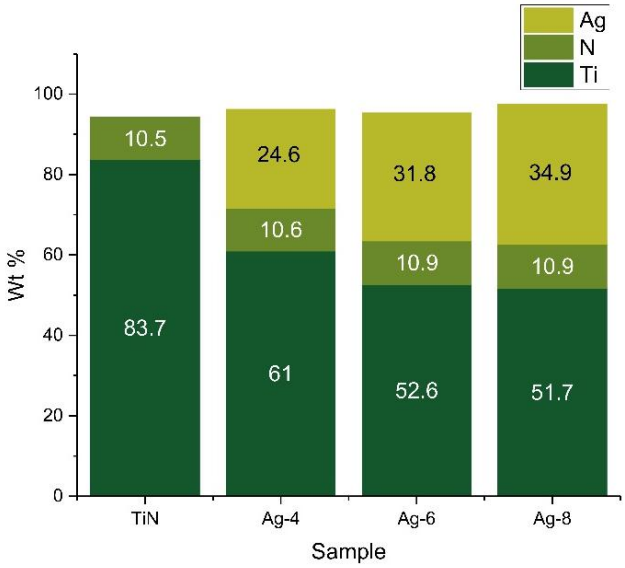

Figure 5 EDS weight percentage of Ti–Ag–N.

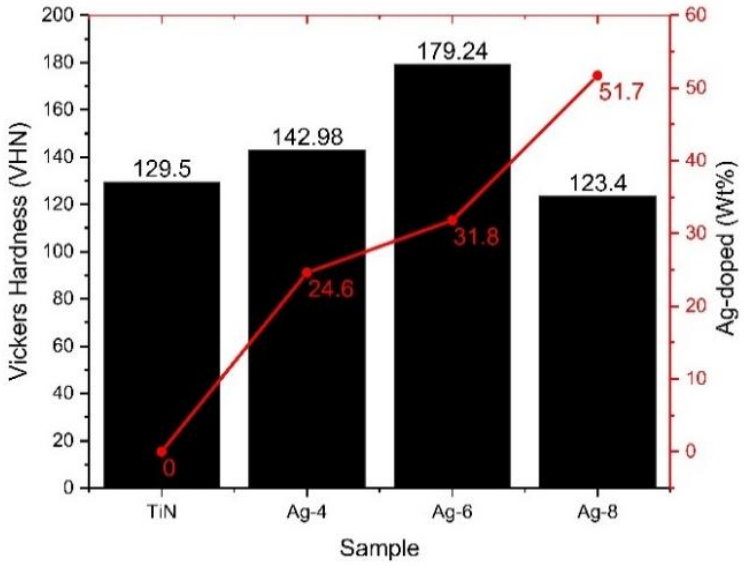

Figure 6 Graphical representation of the effect of Ag content on hardness.

Figure 6 shows that hardness is strongly influenced by Ag content. Undoped TiN records ~129 VHN, which increases to ~143 VHN at Ag-4, suggesting that small Ag additions promote densification and microstructural refinement. The highest hardness is observed at Ag-6 (~179 VHN), indicating an optimal balance where Ag contributes to grain boundary strengthening. The peak hardness at Ag-6 reflects optimal grain boundary strengthening, while the decline at Ag-8 results from both the soft metallic nature of Ag and disruption of grain boundaries due to higher microstrain. At higher loading (Ag-8), hardness falls to ~123 VHN, reflecting embrittlement and phase segregation as Ag behaves like a soft metallic phase within TiN [32]. These results confirm that moderate Ag improves mechanical integrity, while excessive Ag weakens it.

The wettability of Ti–Ag–N surfaces also evolves with time (**Figure 7**). Initial water drops show high contact angles, but within 35 - 60 min they approach zero, indicating a transition to superhydrophilicity. This behavior reflects surface energy changes and possible oxidation, and is consistent with earlier reports where Ag reduced contact angles to ~40°, enhancing biocompatibility [16]. Such time-dependent wetting may help coatings resist biofouling initially while later

supporting tissue integration. Time-resolved measurements (**Figure 8**) confirm Ag's role in tuning wettability. Undoped TiN gradually becomes hydrophilic, while high Ag content (Ag-8) delays wetting. In contrast, Ag-6 shows a sharp drop around 30 min, suggesting that silver concentration can act as a switch for surface energy. Similar phenomena are known in TiO_2 films, where surface restructuring creates hydrophilic sites. For applications, this dual behavior implies that Ag-doped coatings can balance early repellency with long-term compatibility. The transition from hydrophobic to hydrophilic is mainly driven by surface oxidation and Ag-induced restructuring, making it more permanent than simple water adsorption.

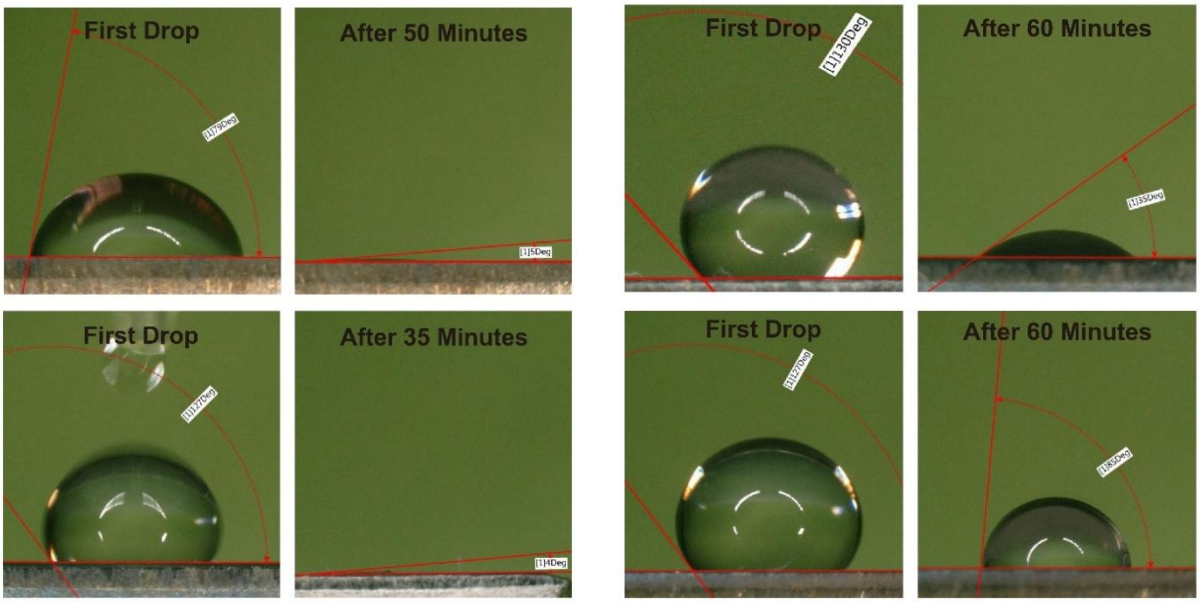

Figure 7 Contact angle images for droplets water on surface sample.

The wettability transition in Ti–Ag–N coatings mainly results from Ag-induced oxidation and surface restructuring. When Ag segregates to the surface, it forms thin Ag_2O or AgO layers that increase surface polarity and enhance water affinity, making the surface more hydrophilic. Moderate Ag levels create uniform oxide coverage and fine surface roughness that promote water spreading, while excessive Ag causes coarse clusters and heterogeneous wetting regions. Thus, controlling Ag content is crucial to balance oxidation, morphology, and surface energy for optimal hydrophilic behavior [15,33,34].

The antibacterial effectiveness data (**Figure 9**) demonstrate that Ti–Ag–N coatings exhibit dramatically improved kill rates against *S. aureus* as silver content increases, with TiN alone reducing bacterial load by only ~52.9%, while Ag-4, Ag-6, and Ag-8 achieve near-complete efficacy 98.9%, 99.98%, and 99.99%, respectively. The corresponding culture images illustrate this trend clearly: Whereas residual bacterial colonies are visible on TiN, Ag-doped surfaces notably diminish colony formation proportionally to Ag content. Such potent antibacterial performance aligns with earlier findings where TiN/Ag multilayer coatings significantly inhibited *S. aureus* proliferation, confirming that silver synergizes with TiN in bactericidal activity [25]. The underlying mechanism, widely supported in the literature, involves the release of Ag^+ ions that disrupt bacterial cell membranes and denature critical proteins and DNA, ultimately leading to cell death [15]. These results underscore the critical role of silver content in optimizing antimicrobial behavior in Ti–Ag–N coatings for biomedical applications. Overall, our data indicate that an Ag concentration of 6 wt% or higher may provide a desirable balance between structural coating properties and superior antibacterial efficacy.

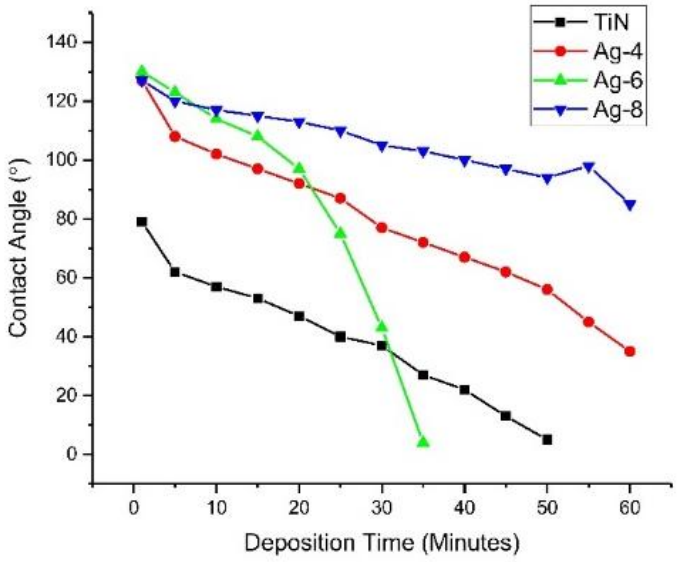

Figure 8 Time-dependent variation of the contact angle.

XRD and SEM–EDS analyses provide direct evidence of Ag segregation, phase separation, and microstrain formation in the Ti–Ag–N coatings. The XRD patterns show that, besides the characteristic TiN peaks, additional reflections corresponding to metallic Ag appear and intensify as Ag content increases, confirming the emergence of a separate Ag phase. The slight shift of TiN peaks toward lower 2θ angles indicates lattice expansion and microstrain, likely caused by atomic-size mismatch between Ti and Ag. SEM–EDS mappings further reveal uniform Ti and N distributions in pure TiN, whereas Ag-containing films display localized Ag-rich regions that become more evident at higher Ag levels, particularly in the Ag-8 sample, signifying Ag segregation and partial phase separation. These findings demonstrate that Ag incorporation modifies the TiN lattice, leading to localized stress and the formation of discrete metallic clusters within the coating matrix.

As Ag concentration increases, distinct structural and compositional transitions occur. EDS data confirm a progressive rise in Ag content, accompanied by reduced TiN crystallite size and enhanced microstrain, both indicative of lattice distortion due to phase segregation. SEM observations reveal gradual grain coarsening and agglomeration with higher Ag levels. Wettability measurements show that moderate Ag incorporation (Ag-6) induces a shift from hydrophobic to hydrophilic behavior, reflecting surface energy modification in TiN/Ag systems. Mechanical testing follows the same pattern: Ag-6 coatings achieve the highest hardness, while Ag-8 exhibits softening, attributed to excessive Ag accumulation that disrupts lattice continuity [35].

Antibacterial evaluations against Staphylococcus aureus confirm that Ag addition significantly enhances bactericidal performance, achieving ~99.98% inhibition for Ag-6 and ~99.99% for Ag-8. This effect arises from the synergistic influence of controlled Ag ion release and surface energy optimization. Collectively, the results indicate that silver acts as a dual-function element: Moderate amounts improve crystallinity, hardness, wettability, and antibacterial efficiency, while excessive addition leads to segregation, softening, and morphological instability. The superior overall performance observed in the Ag-6 sample aligns with prior studies on TiN/Ag multilayers, emphasizing the necessity of balanced Ag incorporation to maintain structural integrity and antimicrobial durability [16]. When precisely optimized, Ti–Ag–N coatings offer a combination of strong mechanical stability, tunable surface energy, and potent antibacterial capability, positioning them as promising materials for advanced food-packaging applications that demand enhanced hygiene and longer product shelf life.

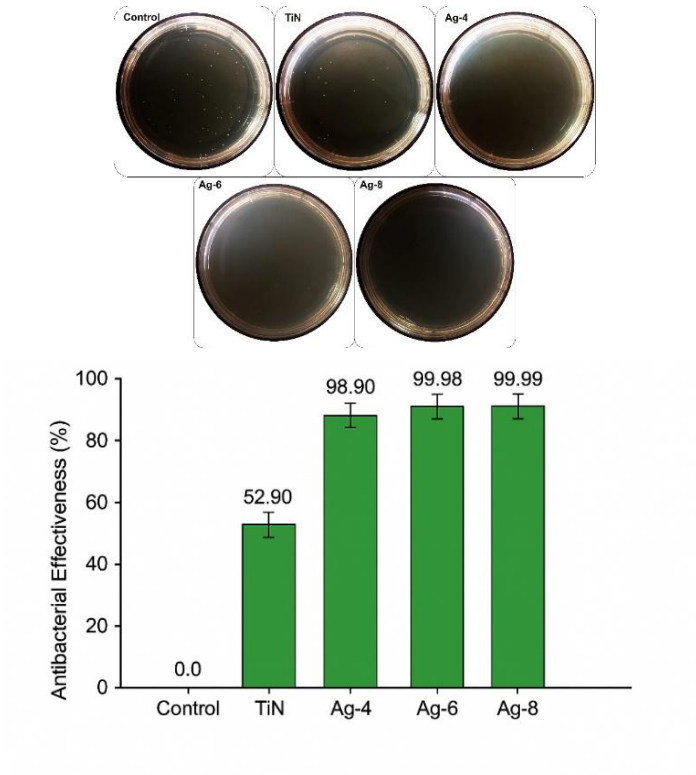

Figure 9 Antibacterial activity analysis: (a) Photographs of colonies in the bacterial growth inhibition test and (b) Antibacterial efficiency.

The quantitative results demonstrate a strong correlation between Ag content, mechanical strength, and antibacterial activity in Ti–Ag–N coatings. Hardness increased from 129.5 VHN for TiN to 179.2 VHN at Ag-6, then decreased to 123.4 VHN at Ag-8, reflecting the dual role of Ag in strengthening and softening the lattice. Moderate Ag incorporation (Ag-6) refined crystallites and introduced beneficial microstrain, while excessive Ag caused segregation and weakened the TiN matrix. Correspondingly, antibacterial effectiveness against S. aureus improved from 52.9% in TiN to 98.9%, 99.98%, and 99.99% for Ag-4, Ag-6, and Ag-8, respectively, indicating a clear enhancement linked to Ag^+ ion release. Preliminary stability observations suggest that Ag-6 maintains a uniform structure with moderate ion diffusion, ensuring long-term performance, whereas Ag-8 shows faster Ag depletion and surface roughening under prolonged liquid exposure. From a safety perspective, controlled Ag levels below ~7 at.% are generally biocompatible, minimizing cytotoxicity while maintaining antibacterial potency. Thus, optimizing Ag concentration is crucial to balance mechanical durability, surface stability, and biological safety, making Ti–Ag–N coatings particularly at Ag-6 composition highly promising for food-packaging and biomedical applications requiring both structural reliability and antimicrobial protection.

Conclusions

This study demonstrates that tailoring the silver content in Ti–Ag–N coatings provides a powerful strategy to optimize their structural, mechanical, surface, and antibacterial properties for multifunctional applications. Moderate Ag incorporation, particularly at Ag-6, achieves a balance between crystallinity, surface energy, and hardness, resulting in enhanced wettability, superior mechanical performance, and nearly complete antibacterial effectiveness against *S. aureus*. In contrast, excessive Ag loading (Ag-8) leads to structural softening and surface instability, although antibacterial performance remains high due to increased Ag ion release. These findings highlight the critical role of controlled Ag concentration in engineering coatings with both long-term mechanical durability and potent antibacterial activity. Overall, the Ti–Ag–N system shows strong potential for advanced biomedical and surface engineering applications, provided that the Ag content is precisely optimized to achieve a synergistic

interplay between structure, surface functionality, and biological performance.

Acknowledgements

This research was supported by the RIIM LPDP Grant and BRIN, grant 272 number B-4131/II.7.5/TK.01.03/02/2025 and B-1703/III.2/TK.01.03/1/2025. We also extend our gratitude to the Research Center for Accelerator Technology - Research Organization for Nuclear Energy.

Declaration of Generative AI in Scientific Writing

The authors declare that generative AI tools were used only to improve the readability and language of the manuscript. These tools were applied with full human oversight and control. The authors remain fully responsible for all scientific content, analysis, and conclusions presented in the paper. No AI tools were listed as authors or co-authors in this work.

CRediT Author Statement

Ihwanul Aziz: Investigation, validation, analysis, data interpretation, and drafted the original manuscript. **Azza Alifa Muhammad:** Data curation. **Frida Iswinning Diah:** Investigation. **Agus Dwiatmaja:** Supervision. **Fajar Sidik Permana:** Software; Validation. **Suharni Suahrni:** Visualization. **Kurnia Wibowo:** Resources; Validation. **Taufik Taufik:** Reviewing and Editing. **Emy Mulyani:** Project administration; Reviewing and Editing.

References

[1] G Shineh, M Mobaraki, MJP Bappy and DK Mills. Biofilm formation, and related impacts on healthcare, food processing and packaging, industrial manufacturing, marine industries and sanitation - A review. *Applied Microbiology* 2023; **3(3)**, 629-665.

[2] Z Li, Q Li, D Ren, X Wu and D Xu. Superhydrophobic surfaces: A promising strategy for addressing food industry challenges. *Innovative Food Science & Emerging Technologies* 2025; **100**, 103899.

[3] RV Wagh, R Priyadarshi, A Khan, Z Riahi, JS Packialakshmi, P Kumar, SN Rindhe and JW Rhim. The role of active packaging in the defense against foodborne pathogens with particular attention to bacteriophages. *Microorganisms* 2025; **13(2)**, 401.

[4] CV Garcia, GH Shin and JT Kim. Metal oxide-based nanocomposites in food packaging: Applications, migration, and regulations. *Trends in Sciences* 2018; **82**, 21-31.

[5] C Echeverria, MDT Torres, M Fernández-García, C de la Fuente-Nunez and A Muñoz-Bonilla. Physical methods for controlling bacterial colonization on polymer surfaces. *Biotechnology Advances* 2020; **43**, 107586.

[6] MA Alsuwat, AA Shah, S Ullah, RU Khan, M Alissa and MS Khan. Microbial biofilm formation to mitigate foodborne pathogens: Strategies and control measures. *Indian Journal of Microbiology* 2025. https://doi.org/10.1007/s12088-025-01461-4

[7] S Zheng, M Bawazir, A Dhall, HE Kim, L He, J Heo and G Hwang. Implication of surface properties, bacterial motility, and hydrodynamic conditions on bacterial surface sensing and their initial adhesion. *Frontiers in Bioengineering and Biotechnology* 2021; **9(1)**, 643722.

[8] M Mu, S Liu, W DeFlorio, L Hao, X Wang, KS Salazar, M Taylor, A Castillo, L Cisneros-Zevallos, JK Oh, Y Min and M Akbulut. Influence of surface roughness, nanostructure, and wetting on bacterial adhesion. *Langmuir* 2023; **39**, 5426-5439.

[9] S Mahmoudi-Qashqay, MR Zamani-Meymian and SJ Sadati. Improving antibacterial ability of Ti-Cu thin films with co-sputtering method. *Scientific Reports* 2023; **13(1)**, 16593.

[10] R Sarvari, B Naghili, S Agbolaghi, S Abbaspoor, H Bannazadeh Baghi, V Poortahmasebi, M Sadrmohammadi and M Hosseini. Organic/polymeric antibiofilm coatings for surface modification of medical devices. *International Journal of Polymeric Materials and Polymeric Biomaterials* 2023; **72**, 867-908.

[11] R Alvarez, S Muñoz-Piña, MU González, I Izquierdo-Barba, I Fernández-Martínez, V Rico, D Arcos, A García-Valenzuela, A Palmero, M Vallet-Regi, AR González-Elipe and JM García-Martín. Antibacterial nanostructured Ti coatings by magnetron sputtering: From laboratory scales

to industrial reactors. *Nanomaterials* 2019; **9(9)**, 1217.

[12] L Bai, R Hang, A Gao, X Zhang, X Huang, Y Wang, B Tang, L Zhao and PK Chu. Nanostructured titanium-silver coatings with good antibacterial activity and cytocompatibility fabricated by one-step magnetron sputtering. *Applied Surface Science* 2015; **355**, 32-44.

[13] A Forte-Castro, JM Pérez, MA Domene, K Ovejero-Paredes, M Filice and I Fernández. Design and characterization of a multifunctional Ag/Ag(I)-coated olive stone material for enhanced preservation and antibacterial protection. *Trends in Sciences* 2025; **49**, 101526.

[14] SM Marques, I Carvalho, TR Leite, M Henriques and S Carvalho. Antimicrobial TiN-Ag coatings in leather insole for diabetic foot. *Materials* 2022; **15(6)**, 2009.

[15] ACS de Arruda, RD Mansano, N Ordonez, R Ruas and SF Durrant. Ag behavior on TiN thin films for decorative coatings. *Coatings* 2024; **14(3)**, 322.

[16] B Petrović, D Mitić, M Miličić Lazić, M Lazarević, A Trajkovska Petkoska, I Nasov, S Živković and V Jokanović. TiN-Ag multilayer protective coatings for surface modification of AISI 316 stainless steel medical implants. *Trends in* Sciences 2025; **15(7)**, 820.

[17] BL Ouay and F Stellacci. Antibacterial activity of silver nanoparticles: A surface science insight. *Nano Today* 2015; **10(3)**, 339-354.

[18] E Nayman, MF Gozukizil, B Armutci, S Temel and FO Gokmen. Structural and gas sensing properties of NiO thin films deposited by a novel spin coating technique. *Journal of Sol-Gel Science and Technology* 2025; **114(2)**, 386-398.

[19] M Yaseen, MAK Khattak, A Khan, S Bibi, M Bououdina, M Usman, NA Khan, AAA Pirzado, RA Abumousa and M Humayun. State-of-the-art electrochromic thin films devices, fabrication techniques and applications: A review. *Nanocomposites* 2023; **10(1)**, 1-40.

[20] SK Mondal, S Chakraborty, S Manna and SM Mandal. Antimicrobial nanoparticles: Current landscape and future challenges. *RSC Pharmaceutics* 2024; **1(3)**, 388-402.

[21] H Zhang, F Li and Q Jia. Preparation of titanium nitride ultrafine powders by sol-gel and microwave carbothermal reduction nitridation methods. *Ceramics International* 2009; **35**, 1071-1075.

[22] SV Kumar, SP Kumar, D Rupesh and K Nitin. Journal of chemical and pharmaceutical research preparations. *International Journal of Current Research in Chemistry and Pharmaceutical Sciences* 2011; **2(3)**, 89-98.

[23] T Elangovan, A Balasankar, S Arokiyaraj, R Rajagopalan, RP George, TH Oh, P Kuppusami and S Ramasundaram. Highly durable antimicrobial tantalum nitride/copper coatings on stainless steel deposited by pulsed magnetron sputtering. *Micromachines* 2022; **13(5)**, 824.

[24] M Truchlý, M Haršáni, A Frkáň, T Fiantok, M Sahul, T Roch, P Kúš and M Mikula. First approach to doping silver into CrB2 thin films deposited by DC/HiPIMS technology in terms of mechanical and tribological properties. *Coatings* 2023; **13(5)**, 824.

[25] S Hojda, M Biegun-Żurowska, A Skórkowska, K Klesiewicz and M Ziąbka. A weapon against implant-associated infections: Antibacterial and antibiofilm potential of biomaterials with titanium nitride and titanium nitride-silver nanoparticle electrophoretic deposition coatings. *International Journal of Molecular Sciences* 2025; **26(4)**, 1646.

[26] UZM Zaidi, AR Bushroa, RR Ghahnavyeh and R Mahmoodian. Crystallite size and microstrain: XRD line broadening analysis of AgSiN thin films. *Pigment & Resin Technology* 2019; **48**, 473-480.

[27] BH Baby and DB Mohan. Structural, optical and electrical studies of DC-RF magnetron co-sputtered Cu, In & Ag doped SnS thin films for photovoltaic applications. *Solar Energy* 2019; **194**, 61-73.

[28] AM Alsaad, AA Ahmad, QM Al-Bataineh, AA Bani-Salameh, HS Abdullah, IA Qattan, ZM Albataineh and AD Telfah. Optical, structural, and crystal defects characterizations of dip synthesized (Fe-Ni) co-doped ZnO thin films. *Materials* 2020; **13(7)**, 1737.

[29] O Kamoun, A Akkari, B Alhalaili, R Vidu and N Turki-Kamoun. Investigations on the synthesis and characterization of silver-doped MoO_3 thin

films for photocatalytic applications. *Scientific Reports* 2025; **15(1)**, 998.

[30] JP Molina-Jiménez, SD Horta-Piñeres, SJ Castillo, JL Izquierdo and DA Avila. Ultra-thin films of CdS doped with silver: Synthesis and modification of optical, structural, and morphological properties by the doping concentration effect. *Coatings* 2025; **15(4)**, 431.

[31] W Tillmann, D Grisales, AM Echavarría, JA Calderón and GB Gaitan. Effect of Ag doping on the microstructure and electrochemical response of TiAlN coatings deposited by DCMS/HiPIMS magnetron sputtering. *Journal of Materials Engineering and Performance* 2022; **31(5)**, 3811-3825.

[32] H Ju, L Yu, D Yu, I Asempah and J Xu. Microstructure, mechanical and tribological properties of TiN-Ag films deposited by reactive magnetron sputtering. *Vacuum* 2017; **141**, 82-88.

[33] I Braceras, M Brizuela, N Álvarez, M Martínez Van Geeteruyen and I Azkona. TiN-Ag as an antimicrobial and wear resistant coating. *Biotribology* 2021; **28**, 100192.